Uncertainty-Aware Multi-View Learning for Prostate Cancer Grading with DWI

Zhicheng Dong[1], Xiaodong Yue[2(✉)], Yufei Chen[3], Xujing Zhou[2], and Jiye Liang[4]

[1] School of Computer Engineering and Science, Shanghai University, Shanghai, China
[2] Artificial Intelligence Institute, Shanghai University, Shanghai, China
yswantfly@shu.edu.cn
[3] College of Electronics and Information Engineering, Tongji University, Shanghai, China
[4] Key Laboratory of Computational Intelligence and Chinese Information Processing of Ministry of Education, School of Computer and Information Technology, Shanxi University, Taiyuan, China

Abstract. Grading of prostate cancer plays an important role in the planning of surgery and prognosis. Multi-parametric magnetic resonance imaging (mp-MRI) of the prostate can facilitate the detection, localization and grade of prostate cancer. In mp-MRI, Diffusion-Weighted Imaging (DWI) can distinguish a malignant neoplasm from benign prostate tissue due to a significant difference in the apparent diffusion sensitivity coefficient (b-value). DWI using high b-value is preferred for prostate cancer grading, providing high accuracy despite a decrease signal-to-noise ratio and increased image distortion. On the other hand, low b-value could avoid confounding pseudo-perfusion effects but in which the prostate normal parenchyma shows a very high signal intensity, making it difficult to distinguish it from prostate cancer foci. To fully capitalize on the advantages and information of DWIs with different b-values, we formulate the prostate cancer grading as a multi-view classification problem, treating DWIs with different b-values as distinct views. Multi-view classification aims to integrate views into a unified and comprehensive representation. However, existing multi-view methods cannot quantify the uncertainty of views and lack a interpretable and reliable fusion rule. To tackle this problem, we propose uncertainty-aware multi-view classification with uncertainty-aware belief integration. We measure the uncertainty of DWI based on Evidential Deep Learning and propose a novel strategy of uncertainty-aware belief integration to fuse multiple DWIs based on uncertainty measurements. Results demonstrate that our method outperforms current multi-view learning methods, showcasing its superior performance.

Keywords: Prostate Cancer Grading · Diffusion-Weighted Imaging · Evidential Multi-View Learning.

1 Introduction

Prostate cancer has emerged as one of the most commonly diagnosed cancers and a major contributor to mortality among men [22]. Accurate grading of prostate cancer is crucial for guiding surgical decisions and predicting prognosis [18, 16]. Diffusion-Weighted Imaging (DWI) plays a pivotal role in prostate cancer grading as it serves as the primary sequence for evaluating prostate cancer in the peripheral zone [26]. The diffusion sensitivity coefficient (b-value) is indicative of the level of diffusion weighting. Typically, many researchers prefer to use a low b-value (500-1000 s/mm^2) since it has high signal-to-noise ratio and can mitigate potential pseudo-perfusion effects [19]. However, the normal prostate parenchyma in DWI with low b-value exhibits a very high signal intensity, posing a challenge in distinguishing it from prostate cancer foci [13]. On the other hand, high b-value (1500-2000 s/mm^2) can improve the contrast between tumor and normal tissue but lead to a reduction in signal-to-noise ratio [4]. This inspired us to effectively integrate DWIs using different b-values to achieve precise grading of prostate cancer.

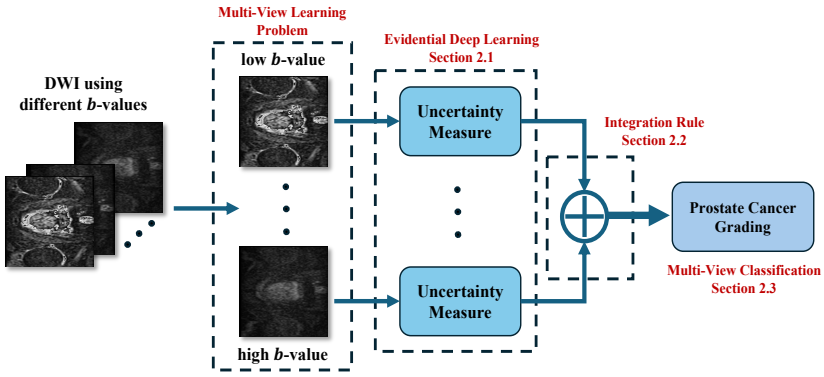

Fig. 1. The workflow of multi-view fusion based on uncertainty measurement.

Multi-view classification has been proven to be effective in integrating various sources to enhance classification accuracy [10, 2, 8, 1, 20, 3, 5]. Due to the multi-view learning method can adaptively integrate correlational information from different views, many multi-view methods have been proposed for the grading, staging and segmentation of cancer using US, CT or MRI [15, 27, 6, 25, 11]. Therefore, it's nature to apply multi-view learning to fuse DWIs with multiple b-values. However, the relevant work for fuse DWIs is limited and the current multi-view learning methods cannot measure the uncertainty associated with each view, i.e., the reliability of DWIs with different b-values and their integration rule lacks interpretability, rendering them unreliable for prostate cancer grading.

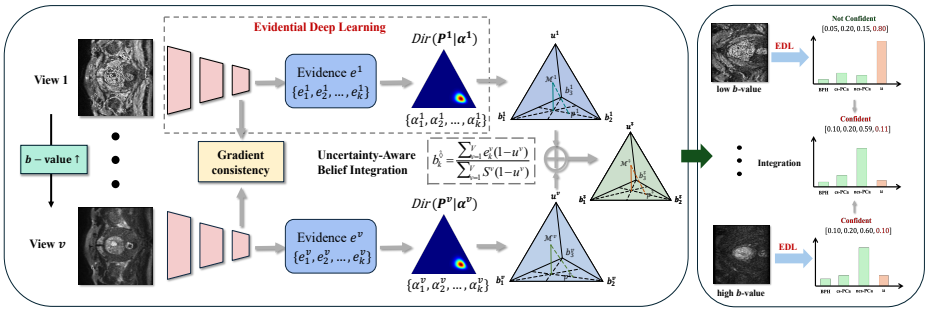

Fig. 2. Module overview. The overall process of the proposed method can be divided into two steps: (1) The view-specific evidential neural network learns evidence and use subjective logic to form uncertainty and uncertainty-aware belief integration is employed to fuse results from multiple DWIs. (2) During the testing phase, we not only obtain an interpretable fusion result but also discern the reliability of DWIs with different b-values using our method.

To address the problem above, we innovatively apply multi-view learning to integrate DWIs with b-values for the prediction of prostate cancer grading and integrate the multi-view classification with the theory of evidential uncertainty measurement. Based on Evidential Deep Learning (EDL) [23], we assess the uncertainty of DWIs with different b-values. On these grounds, we introduce an innovative fusion strategy of uncertainty-aware belief integration, which integrates views directly based on their uncertainty measurements. In this way, we can assess the reliability of each specific DWI with a certain b-value and obtain interpretable fusion results. The contributions of this paper are summarized below.

(1) We apply deep multi-view learning to the fusion of prostate cancer DWIs with multiple b-values, which can enhance the accuracy of prostate cancer grading.
(2) We incorporate uncertainty measure into the deep multi-view learning, rendering the DWI fusion interpretable and evaluate the reliability of the imaging under different b-values.

2 Method

The workflow and overview of our method is illustrated in Figure 1 and 2. Initially, we formulate prostate cancer grading with DWIs using different b-values as a multi-view learning problem. Furthermore, we employ the Evidential Deep Learning (EDL) [23] to formulate the Dirichlet distribution and the opinion for each view (b-value). Subsequently, we adopt uncertainty-aware belief fusion to integrate opinions from multiple views. As a result, we can obtain the fusion results for prostate cancer grading.

2.1 Uncertainty Measure of Data Views

Referring to the aforementioned, we apply Evidential deep learning to quantify the uncertainty of DWIs with different b-values, enabling uncertainty-aware multi-view fusion. Specifically, given a DWI x^v under b^v-value $v \in \{1, 2, ..., V\}$ (lower sequence indices v correspond to lower b-value), EDL assumes a Dirichlet distribution $Dir(\boldsymbol{P}^v|\boldsymbol{\alpha}^v)$ to model the distribution of categorical probability $\boldsymbol{P}^v \in \mathbb{R}^K$, where $\boldsymbol{\alpha}^v \in \mathbb{R}^K$ is the parameters of Dirichlet distribution. After that, the opinion $\mathcal{M}^v = \{\{b_k^v\}_{k=1}^K, u^v\}$ can be derived based on Subjective Logic [12], denoted as

$$b_k^v = \frac{\alpha_k^v - 1}{S^v} = \frac{e_k^v}{S^v}, \quad u^v = \frac{K}{S^v}, \tag{1}$$

where e_k^v is the non-negative evidence collected from kth class by EDL and $S^v = \sum_{k=1}^K \alpha_k^v$ represents the Dirichlet strength. The EDL is trained by minimizing the negated logarithm of the marginal likelihood, given by

$$\mathcal{L}_{nll}(\boldsymbol{\alpha}_i^v) = \sum_{k=1}^{K} y_{ik} \left(\log\left(S_i^v\right) - \log\left(\alpha_{ik}^v\right) \right), \tag{2}$$

for a sample x_i containing multiple DWIs with different b-values of class k, y_{ik} is the one-hot vector encoding the ground-truth class of x_i, $y_{ik} = 1$ and $y_{ij} = 0$ for all $j \neq k$, $\boldsymbol{\alpha}_i^v$ is the parameters of Dirichlet distribution of x_i belonging to K classes on b^v-value.

The objective of EDL only ensures higher evidence for the correct class, ignoring low evidences for incorrect classes, leading to unreasonably low uncertainty. We address this by introducing KL divergence, denoted as

$$\mathcal{L}_{kl}\left(\widetilde{\boldsymbol{\alpha}}_i^v\right) = KL\left(Dir\left(\boldsymbol{p}_i^v \mid \widetilde{\boldsymbol{\alpha}}_i^v\right) \| Dir\left(\boldsymbol{p}_i^v \mid \mathbf{1}\right)\right), \tag{3}$$

where $\widetilde{\boldsymbol{\alpha}}_i^v = \boldsymbol{y}_i + (\mathbf{1} - \boldsymbol{y}_i) \odot \boldsymbol{\alpha}_i$ is the adjusted Dirichlet parameters. Finally, the objective for a single DWI is

$$\mathcal{L}(\boldsymbol{\alpha}_i^v) = \mathcal{L}_{nll}(\boldsymbol{\alpha}_i^v) + \lambda_t \mathcal{L}_{kl}\left(\widetilde{\boldsymbol{\alpha}}_i^v\right) \tag{4}$$

where $\lambda_t = min\{1, t/10\}$ is the the annealing coefficients to prevent the model from learning a uniform Dirichlet distribution in the early stage of training.

2.2 Uncertainty-Aware Multi-View Belief Integration

Based on the derivation of belief mass and uncertainty measure, we propose a novel fusion rule named *Uncertainty-Aware Belief Integration* to obtain the fusion results of multi-view DWIs with different b-values.

Definition 1. ***Uncertainty-Aware Belief Integration.*** *Specifically, given a data composed of V multiple views (DWIs under v b-values), the final opinion $\mathcal{M} = \{\{b_k^{\diamond}\}_{k=1}^K, u^{\diamond}\}$ after integration can be calculated from the opinion $\mathcal{M}^v =$*

$\{\{b_k^v\}_{k=1}^K, u^v\}$ *collected by each view-specific neural network, which can be written as*

$$b_k^{\widehat{\diamond}} = \frac{e_k^{\widehat{\diamond}}}{S} = \frac{\frac{\sum_{v=1}^V e_k^v(1-u^v)}{\sum_{v=1}^V(1-u^v)}}{\frac{\sum_{k=1}^K\sum_{v=1}^V e_k^v(1-u^v)}{\sum_{v=1}^V(1-u^v)} + K} = \frac{\sum_{v=1}^V e_k^v(1-u^v)}{\sum_{v=1}^V S^v(1-u^v)}, \tag{5}$$

$$u^{\widehat{\diamond}} = \frac{K}{S} = \frac{K}{\frac{\sum_{k=1}^K\sum_{v=1}^V e_k^v(1-u^v)}{\sum_{v=1}^V(1-u^v)} + K} = \frac{\sum_{v=1}^V(1-u^v)}{\sum_{v=1}^V(\frac{1}{u^v}-1)}. \tag{6}$$

Proposition 1. *Incorporating a DWI with high uncertainty ($u^v \to 1$) into the original fusion result cannot significantly impact the integrated uncertainty.*

Proof. Let $\delta \to 0^+$ be the sum of evidence given by the new DWI with high uncertainty ($u^v \to 1$), we have

$$\lim_{\delta\to 0^+} \widetilde{u}^{\widehat{\diamond}} = \lim_{\delta\to 0^+} \frac{\sum_{v=1}^V(1-u^v) + \frac{\delta}{\delta+K}}{\sum_{v=1}^V(\frac{1}{u^v}-1) + \frac{\delta}{K}} = \frac{\sum_{v=1}^V(1-u^v)}{\sum_{v=1}^V(\frac{1}{u^v}-1)} = u^{\widehat{\diamond}}. \tag{7}$$

This proposition means that our method assigns weights dynamically based on the uncertainty of DWI with different b-values.

Proposition 2. *Let $u^{\widehat{\diamond}}$ be the integrated uncertainty after belief combination, $\{u^v\}_{v=1}^V$ be the uncertainty from V views, we have $u_{min} \le u^{\widehat{\diamond}} \le u_{max}$, where $u_{max} = \max\{u^v\}_{v=1}^V$ and $u_{min} = \min\{u^v\}_{v=1}^V$.*

Proof.

$$u^{\widehat{\diamond}} \ge \frac{\sum_{v=1}^V(1-u^v)}{\sum_{v=1}^V(\frac{1-u^v}{u_{\min}})} = u_{\min} \tag{8}$$

$$u^{\widehat{\diamond}} \le \frac{\sum_{v=1}^V(1-u^v)}{\sum_{v=1}^V(\frac{1-u^v}{u_{\max}})} = u_{\max} \tag{9}$$

This range ensures the quality of the integrated uncertainty measurement in the context of prostate cancer grading, reducing the challenges caused by extremely low or high b-values like confounding pseudo-perfusion effect or high signal intensity.

To alleviate the conflict between views, we enhance our proposed method by introducing a cross view conflict regulation. We use an exponential evidence function to predict the evidence for each view, i.e., $\boldsymbol{e}_i^v = \exp(\boldsymbol{z}_i^v)$ where $\boldsymbol{z}_i^v$ is the logits produced by the last layer. The gradient g_{ik}^v of $\mathcal{L}_{nll}(\boldsymbol{\alpha}_i^v)$ belonging to kth class can be derived

$$g_{ik}^v = \nabla_{\boldsymbol{z}_{ik}^v} \mathcal{L}_{nll}\left(\boldsymbol{\alpha}_i^v\right) = y_{ik}\left[\frac{S_i^v - K\alpha_{ik}^v}{S_i^v \alpha_{ik}^v}\right] = y_{ik}\left[\frac{1}{\alpha_{ik}^v} - u_i^v\right]. \tag{10}$$

We see that the gradient will be scaled depending on the uncertainty and how much Dirichlet parameter α_{ik}^v is placed on the correct class. We minimize the discrepancy between these different gradient vectors. The consistency regulation loss is derived as

$$\mathcal{L}_{cons}(\{\boldsymbol{\alpha_i^v}\}_{v=1}^V) = \sum_{v=1}^{V-1} \sum_{m=v+1}^{V} \left|\left|g_i^v - g_i^m\right|\right|, \tag{11}$$

by which the gradients of different views are aligned.

To simultaneously foster reasonable opinions across all views, we employ a multi-task strategy with an integrated loss function

$$\mathcal{L}_{overall} = \sum_{i=1}^{N}\left[\sum_{v=1}^{V} \mathcal{L}(\boldsymbol{\alpha_i^v}) + \mathcal{L}(\boldsymbol{\alpha}_{\boldsymbol{i}}^{\hat{\diamond}}) + \lambda \mathcal{L}_{cons}(\{\boldsymbol{\alpha_i^v}\}_{v=1}^V)\right]. \tag{12}$$

where $\lambda = 0.1$ denotes the trade-off hyper-parameter.

3 Experiments

3.1 Dataset and Implementation Details

We apply our method to a real-world prostate cancer DWI dataset collected by Ma'anshan People's Hospital. The dataset consist of 134 patients with benign prostatic hyperplasia (BPH), 37 patients with clinically significant prostate cancer (cs-PCa), 64 patients with non-clinically significant prostate (ncs-PCa) cancer. For all patients, we obtained their DWIs with b-values of 500, 1500 and 2000 s/mm^2, serving as three views for model input. The total number of DWIs from each b-value is 2144. Our method utilized ResNet18 [9] as our feature extractor for all views. The Adam optimizer [14] with an $l2$-norm regularization set at 1e-5 is employed to train the whole framework. The learning rate is determined through a 5-fold cross-validation procedure, selecting from the learning rate candidates: {1e-4, 3e-4, 1e-3, 3e-3}. The whole framework is implemented by PyTorch on one NVIDIA TITAN Xp with GPU of 12GB memory.

Table 1. Comparison with state-of-the-art multi-view learning methods. The best results are bolded and the second best results are underlined.

Method	ACC	AUC	ECE	F1-Score
Early Fusion	80.33±1.01	85.93±1.96	0.151±0.011	72.17±0.45
DCCAE [24]	79.33±2.14	82.34±1.17	0.174±0.059	70.77±0.68
TMC [7]	<u>83.04±0.37</u>	<u>91.98±0.63</u>	<u>0.078±0.046</u>	72.50±0.91
SMDC [17]	82.98±0.52	86.70±1.40	0.094±0.73	<u>74.63±1.29</u>
Ours	**86.70±0.54**	**93.39±0.99**	**0.073±0.013**	**80.26±0.43**

Table 2. Ablation study, "✓" means ours with the corresponding component, "-" means "not applied".

Main Components			Metric	
Fusion	$\mathcal{L}_{cons}$	$\mathcal{L}_{kl}$	ACC	AUC
-	-	-	72.20	82.37
✓	-	-	82.91	85.97
✓	✓	-	84.23	<u>92.99</u>
✓	-	✓	<u>84.45</u>	92.03
✓	✓	✓	**86.70**	**93.39**

3.2 Test of Improvement with Multi-View Fusion

In this section, we experimentally validated the effectiveness of our fusion method compared to different multi-view learning methods and solely using a single b-value and conduct ablation study.

Results shown in Table 1 show that our method outperforms all methods in terms of different metrics. For example, our method improves the accuracy and AUC by about 6.37% and 7.46% compared to Early Fusion, indicating that the quality of uncertainty measurement for each view obtained by our method is high, leading to better outcomes after uncertainty-aware integration. Furthermore, the test ECE of our method outperforms all, indicating our model has been well calibrated.

Furthermore, We perform the experiments to investigate the effectiveness of KL divergence and cross-view gradient regulation. As shown in Table 2, it is obvious that all the components we proposed contribute to the improvement of the model's performance. Furthermore, we compare our method with those solely using single b-value DWI for grading. The results in Fig. 3 (a) indicate that our method could exploit and integrate information from DWIs with multiple b-values, enhancing the performance of prostate cancer grading.

3.3 Measure Uncertainty of DWIs with b-values

In this test, we measure the uncertainty of DWIs with different b-values and present some typical examples.

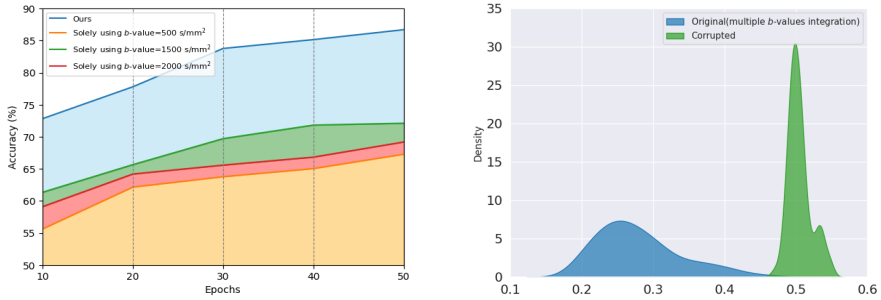

(a) Classification Performance Comparison. (b) Uncertainty Estimation.

Fig. 3. (a) The curves in blue and other color correspond to accuracy of our method integrating DWIs under multiple b-values and ResNet18 solely using single b-value. (b) Uncertainty estimation after integration. Blue represents the original DWI dataset, and green represents DWIS after adding gaussian noise.

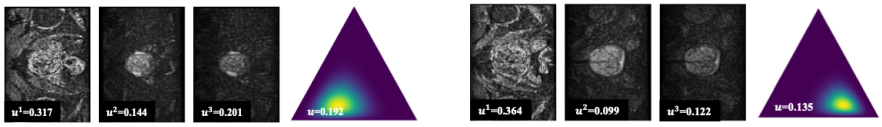

(a) cs-PCa. (b) ncs-PCa.

Fig. 4. Typical samples of cs-PCa (a) and ncs-PCa (b). Uncertainties of DWIs with multiple b-values have been estimated by our model. u^1, u^2 and u^3 correspond to DWIs with b-value = 500, 1500 and 2000 s/mm^2, respectively. Please refer to supplementary materials for more typical examples

First, we estimate the integrated uncertainty on the modified dataset, in which we added gaussian noise to all DWIs. The Gaussian kernel density estimation [21] of learned uncertainty is shown in Fig. 3 (b). It can be found that the estimated uncertainty is closely related to the quality of DWI, validating that our method are aware of the quality of DWI with each b-value.

Next, we present two typical examples to validate the effectiveness of our fusion method in terms of uncertainty estimation. As show in Fig. 4, because the tumor regions of prostate cancer are challenging to distinguish on low b-value DWI and high b-value DWI has a high signal-to-noise ratio and low image quality, DWI with extremely low b-value (500 s/mm^2) and high b-value (2000 s/mm^2) tend to have higher uncertainty, demonstrating that our approach can accurately measure the uncertainty of DWI.

4 Conclusion

In this paper, we introduce a uncertainty-aware multi-view learning method for prostate cancer grading. Utilizing Evidential Deep Learning, we formulate the

uncertainty of DWIs with various b-values based on Subjective Logic. Furthermore, our proposed uncertainty-aware belief fusion focuses on exploring and exploiting the uncertainty obtained by EDL. As a result, we can not only capture the uncertainty of DWIs with different b-values and the fusion results are interpretable.

Acknowledgments. This work was supported by the National Natural Science Foundation of China (Serial Nos. 62173252, 61976134) and Natural Science Foundation of Shanghai, China (Serial No. 21ZR1423900).

Disclosure of Interests. The authors have no competing interests to declare that are relevant to the content of this article.

References

1. Andrew, G., Arora, R., Bilmes, J., Livescu, K.: Deep canonical correlation analysis. In: International conference on machine learning. pp. 1247–1255. PMLR (2013)
2. Bach, F.R., Jordan, M.I.: Kernel independent component analysis. Journal of machine learning research **3**(Jul), 1–48 (2002)
3. Bachman, P., Hjelm, R.D., Buchwalter, W.: Learning representations by maximizing mutual information across views. Advances in neural information processing systems **32** (2019)
4. Barrett, T., Priest, A.N., Lawrence, E.M., Goldman, D.A., Warren, A.Y., Gnanapragasam, V.J., Sala, E., Gallagher, F.A.: Ratio of tumor to normal prostate tissue apparent diffusion coefficient as a method for quantifying dwi of the prostate. American Journal of Roentgenology **205**(6), W585–W593 (2015)
5. Chen, T., Kornblith, S., Norouzi, M., Hinton, G.: A simple framework for contrastive learning of visual representations. In: International conference on machine learning. pp. 1597–1607. PMLR (2020)
6. Gao, Z., Liu, Y., Wu, F., Shi, N., Shi, Y., Zhuang, X.: A reliable and interpretable framework of multi-view learning for liver fibrosis staging. arXiv preprint arXiv:2306.12054 (2023)
7. Han, Z., Zhang, C., Fu, H., Zhou, J.T.: Trusted multi-view classification. In: International Conference on Learning Representations (2020)
8. Hardoon, D.R., Shawe-Taylor, J.: Sparse canonical correlation analysis. Machine Learning **83**, 331–353 (2011)
9. He, K., Zhang, X., Ren, S., Sun, J.: Deep residual learning for image recognition. In: Proceedings of the IEEE conference on computer vision and pattern recognition. pp. 770–778 (2016)
10. Hotelling, H.: Relations between two sets of variates. In: Breakthroughs in statistics: methodology and distribution, pp. 162–190. Springer (1992)
11. Huang, X., Yue, X., Xu, Z., Chen, Y.: Harnessing deep bladder tumor segmentation with logical clinical knowledge. In: International Conference on Medical Image Computing and Computer-Assisted Intervention. pp. 725–735. Springer (2022)
12. Jøsang, A.: Subjective logic, vol. 3. Springer (2016)
13. Kim, C.K., Park, B.K., Kim, B.: High-b-value diffusion-weighted imaging at 3 t to detect prostate cancer: comparisons between b values of 1,000 and 2,000 s/mm2. American Journal of Roentgenology **194**(1), W33–W37 (2010)

14. Kingma, D.P., Ba, J.: Adam: A method for stochastic optimization. arXiv preprint arXiv:1412.6980 (2014)
15. Kwak, J.T., Hewitt, S.M.: Multiview boosting digital pathology analysis of prostate cancer. Computer methods and programs in biomedicine **142**, 91–99 (2017)
16. Litwin, M.S., Tan, H.J.: The diagnosis and treatment of prostate cancer: a review. Jama **317**(24), 2532–2542 (2017)
17. Liu, W., Chen, Y., Yue, X., Zhang, C., Xie, S.: Safe multi-view deep classification. In: Proceedings of the AAAI Conference on Artificial Intelligence. vol. 37, pp. 8870–8878 (2023)
18. Manenti, G., Nezzo, M., Chegai, F., Vasili, E., Bonanno, E., Simonetti, G., et al.: Dwi of prostate cancer: optimal-value in clinical practice. Prostate Cancer **2014** (2014)
19. Merisaari, H., Toivonen, J., Pesola, M., Taimen, P., Boström, P.J., Pahikkala, T., Aronen, H.J., Jambor, I.: Diffusion-weighted imaging of prostate cancer: effect of b-value distribution on repeatability and cancer characterization. Magnetic Resonance Imaging **33**(10), 1212–1218 (2015)
20. Morvant, E., Habrard, A., Ayache, S.: Majority vote of diverse classifiers for late fusion. In: Structural, Syntactic, and Statistical Pattern Recognition: Joint IAPR International Workshop, S+ SSPR 2014, Joensuu, Finland, August 20-22, 2014. Proceedings. pp. 153–162. Springer (2014)
21. Ramsay, P.H.: Multivariate density estimation, theory, practice, and visualbation (1993)
22. Rawla, P.: Epidemiology of prostate cancer. World journal of oncology **10**(2), 63 (2019)
23. Sensoy, M., Kaplan, L., Kandemir, M.: Evidential deep learning to quantify classification uncertainty. Advances in neural information processing systems **31** (2018)
24. Wang, W., Arora, R., Livescu, K., Bilmes, J.: On deep multi-view representation learning. In: International conference on machine learning. pp. 1083–1092. PMLR (2015)
25. Wang, Y., Li, Z., Mei, J., Wei, Z., Liu, L., Wang, C., Sang, S., Yuille, A.L., Xie, C., Zhou, Y.: Swinmm: masked multi-view with swin transformers for 3d medical image segmentation. In: International Conference on Medical Image Computing and Computer-Assisted Intervention. pp. 486–496. Springer (2023)
26. Woo, S., Suh, C.H., Kim, S.Y., Cho, J.Y., Kim, S.H.: Head-to-head comparison between high-and standard-b-value dwi for detecting prostate cancer: a systematic review and meta-analysis. Ajr Am J Roentgenol **210**(1), 91–100 (2018)
27. Zhang, K., Zhuang, X.: Shapepu: A new pu learning framework regularized by global consistency for scribble supervised cardiac segmentation. In: International Conference on Medical Image Computing and Computer-Assisted Intervention. pp. 162–172. Springer (2022)